Article

Nature of Minor-Groove Binders–DNA Complexes in the Gas Phase

Manuel Rueda, Luque, and Modesto Orozco

J. Am. Chem. Soc., **2005**, 127 (33), 11690-11698• DOI: 10.1021/ja0422110 • Publication Date (Web): 27 July 2005

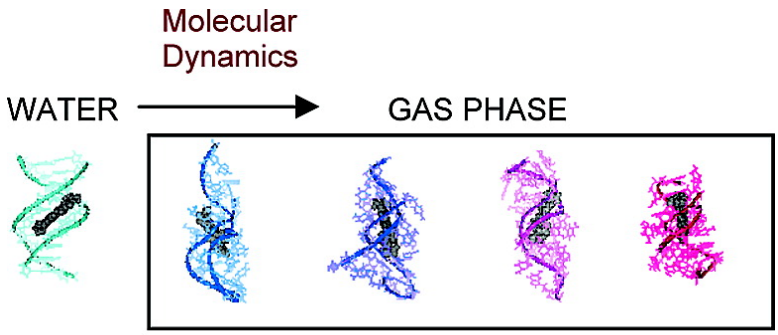

Minor groove binders

More About This Article

Additional resources and features associated with this article are available within the HTML version:

- Supporting Information
- Links to the 3 articles that cite this article, as of the time of this article download
- Access to high resolution figures
- Links to articles and content related to this article
- Copyright permission to reproduce figures and/or text from this article

View the Full Text HTML

J|A|C|S
ARTICLES
Published on Web 07/27/2005

Nature of Minor-Groove Binders−DNA Complexes in the Gas Phase

Manuel Rueda,[†,‡] F.Javier Luque,*[,§] and Modesto Orozco*[,†,‡]

Contribution from the Institut de Recerca Biomédica, Parc Científic de Barcelona, Josep Samitier 1-5, Barcelona 08028, Spain, Departament de Bioquímica i Biología Molecular, Facultat de Química, Universitat de Barcelona, Martí i Franqués 1, Barcelona 08028, Spain, and Departament de Fisicoquímica, Facultat de Farmacia, Universitat de Barcelona, Avgda Diagonal 643, Barcelona 08028, Spain

Received December 27, 2004; E-mail: modesto@mmb.pcb.ub.es; fjluque@ub.edu

Abstract: The structure of noncovalent complexes of DNA duplex with minor groove binders (mG-binders) has been analyzed by *state of the art* molecular dynamics (MD) simulations. More than 3.3 μs of MD trajectories (including 4×0.5 μs trajectories) were collected for the Dickerson's dodecamer bound to DAPI, Hoechst 33258, and Netropsin. Comparison of these trajectories with control simulations in water allowed us to determine that the extreme dehydration and partial neutralization occurring during electrospray experiments does not produce the disruption of the DNA:mG-binder complexes or the dissociation of the two strands of the duplex. Irrespective of the drug and the simulation conditions the mG-binders remains bound to the DNA near the preferential binding position in aqueous conditions. Large distortions appear in the two DNA strands, which maintain however a memory of the original DNA duplex structure in water, and a general helical-like conformation.

Introduction

The physiological structure of DNA[1−4] is determined by five major interactions: (i) intra-strand covalent bond, (ii) intra- and interstrand stacking, (iii) interstrand hydrogen bonds (H-bonds), (iv) phosphate−phosphate repulsion, and (v) solvent interactions. Polar solvents such as water disfavor base recognition, since the unpaired bases are better solvated than the stacked and hydrogen-bonded base pairs, but are crucial[5−7] to screen the very large phosphate−phosphate repulsion. Thus, for a typical interphosphate distance along the minor groove the repulsion energy in the gas phase between two nucleotides in B-DNA is around 30 kcal/mol. Accordingly, one could expect that in absence of water the DNA will unfold. Nevertheless, electrospray (ES) data suggest[8−17] that the DNA can adopt a duplex structure in the gas phase. These findings have been recently supported by molecular dynamics (MD) simulations performed in our laboratory, which showed that under conditions similar to those of the ES experiment the DNA retains a good structural and dynamical memory of the duplex in water.[18] Our simulations also suggested that 12- and 16-mer DNA duplexes maintain a distorted helical conformation in the gas phase, keeping some memory of the original helical structure in solution.[18] Very recently Bower's group performed experimental cross-section measures combined with 2 ns MD simulations,[17] confirming that helical and not globular conformations are the dominant ones in ES experiments of medium and large DNA duplexes.

ES experiments of noncovalent DNA−drug complexes have suggested that these complexes survive vaporization.[8−12,14−16] Moreover, for a given sequence the amount of drug−DNA complex in the gas phase increases as the affinity of the drug for the DNA in water does.[11,12,14−16] These findings are quite surprising, especially for minor groove binders (mG-binders), since their (quite external) interaction with DNA strongly depends on the existence of a B-type conformation in the duplex. Then, one might reasonably expect that the structural changes

† Parc Científic de Barcelona.
‡ Facultat de Química, Universitat de Barcelona.
§ Departament de Fisicoquímica, Facultat de Farmacia, Universitat de Barcelona.

(1) Watson, J. D.; Crick, F. H. C. *Nature* **1953**, *171*, 1303−1324.
(2) Saenger, W. *Principles of Nucleic Acid Structure*; Springer-Verlag: New York, 1984; pp 2−457.
(3) Blackburn, G. M.; Gait, M. J. *Nucleic Acids in Chemistry and Biology*; IRL Press: Oxford, 1990; pp 17−70.
(4) Bloomfield, V. A.; Crothers, D. M.; Tinoco, I. *Nucleic Acids. Structure, Properties and Functions.* University Science Books: Sausalito, CA, 2000; pp 165−217.
(5) Herskovits, T. T.; Harrington, J. P. *Biochemistry* **1972**, *11*, 4800−4811.
(6) Levine, L.; Gordon, J. A.; Jencks, W. P. *Biochemistry* **1963**, *2*, 168−175.
(7) Turner, D. H. In *Nucleic Acids. Structure, Properties and Functions*; Bloomfield, V. A.; Crothers, D. M.; Tinoco, I., Eds.; University Science Books: Sausalito, CA, 2000; pp 308−310.
(8) Gale, D. C.; Smith, R. D. *J. Am. Soc. Mass. Spectrom.* **1995**, *6*, 1154−1164.
(9) Hofstadler, S. A.; Griffey, R. H. *Chem. Rev.* **2001**, *101*, 377−390.
(10) Gabelica, V.; De Pauw, E. *J. Mass Spectrom.* **2002**, *219*, 151−159.
(11) Gabelica, V.; De Pauw, E.; Rosu, F. *J. Mass. Spectrom.* **1999**, *34*, 1328−1337.
(12) Wan, K. X.; Shibue, T.; Gro, M. L. *J. Am. Chem. Soc.* **2000**, *122*, 300−307.
(13) Reyzer, M. L.; Brodbelt, J. S.; Kerwin, S. M.; Kuman, D. *Nucleic Acids Res.* **2001**, *29*, 103−116.
(14) Gabelica, V.; Rosu, R.; Houssier, C.; De Pauw, E. *Rapid Commun. Mass Spectrom.* **2000**, *14*, 464−467.
(15) Rosu, F.; Valerica, G.; Houssier, C.; De Pauw, E. *Nucleic Acids Res.* **2002**, *30*, e82.
(16) Gabelica, V.; De Pauw, E. *J. Mass Spectrom.* **2001**, *36*, 397−402.
(17) Gidden, J.; Ferzoco, A.; Baker, E. S.; Bowers, M. T. *J. Am. Chem. Soc.* **2004**, *126*, 15132−15140.
(18) Rueda, M.; Kalko, S. G.; Luque, F. J.; Orozco, M. *J. Am. Chem. Soc.* **2003**, *125*, 8007−8014.

10.1021/ja0422110 CCC: $30.25

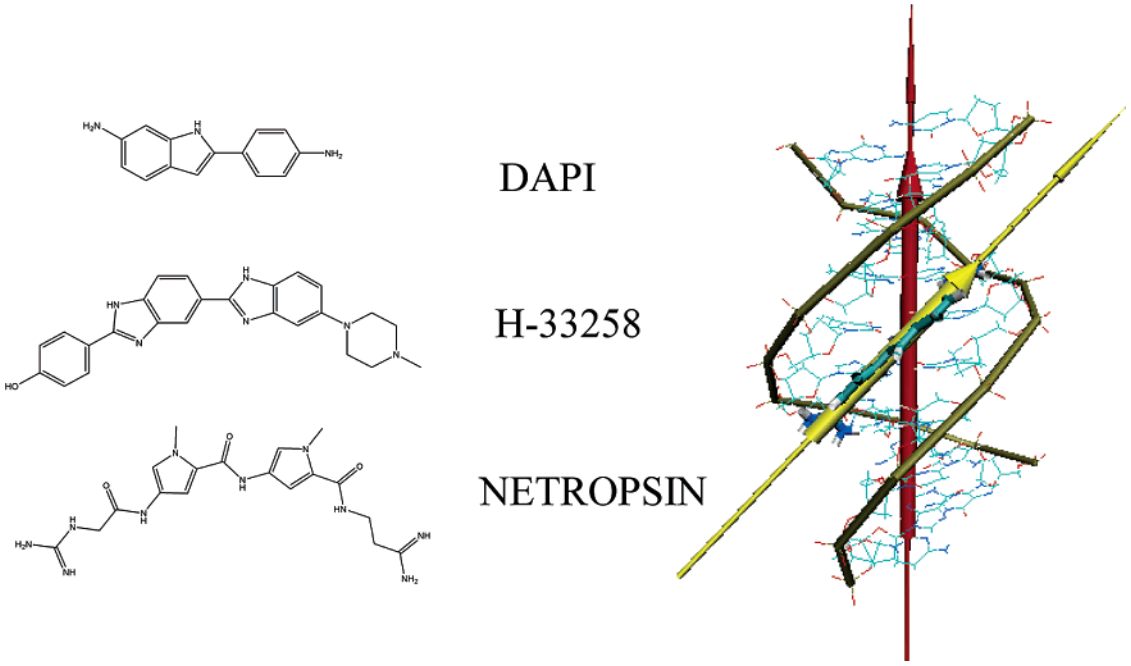

Figure 1. Local reference system used to describe the relative positioning of drug and DNA. The center-of-mass and the *z*-axis for drugs and DNA are derived by calculation of inertia moments for each snapshot. The orientation is measured from the angle formed between the *z*-axis of drug and DNA.

induced in the DNA upon dehydration would affect its ability to accommodate the mG-binder and eventually be difficult or even impede the binding of the drug in the minor groove. The disagreement between chemical intuition and the overwhelming experimental evidence is then evident.

In this paper we present a systematic study of the structure and dynamics of complexes of DNA with three well-known mG-binders: DAPI, Hoechst 33258, and Netropsin. Very large trajectories (up to 0.5 μs long) of the drug:DNA duplexes in the gas phase have been performed under different simulation conditions and compared with those obtained for the naked DNA and for those corresponding to aqueous solution. The results, obtained after more than 3.3 μs of *state-of-the-art* MD simulations, allowed us to describe for the first time, to the best of our knowledge, the nature of mG-binders:DNA interactions in the gas phase.

Methods

We have analyzed the structure of the complexes of Drew–Dickerson's dodecamer d(CGCGAATTCGCG)[19] with DAPI,[20] Hoechst 33258,[21] and Netropsin[22] (see Figure 1), which bind to the B-type DNA in A-rich regions. The crystal structures of their complexes with Dickerson's dodecamer are deposited in the Protein Data Bank with codes 1d30 (DAPI), 1d43 (Hoechst 33258), and 1d86 (Netropsin) (see refs 20–22). The three structures were solved with a similar resolution (2.0–2.4 Å) and show how the drugs are placed in the minor groove of the central AATT without inducing dramatic distortions in the structure of the duplex.

Control MD Simulations in Water. The starting structures of the complexes were immersed in a polyhedral box containing around 4000 water molecules. The systems were neutralized by adding 22 sodium and 1 (Hoechst 33258) or 2 (DAPI, Netropsin) chlorine ions. We used the iterative cMIP[23] procedure to locate first the Cl^- anions near the drug and subsequently the Na^+ cations near the phosphates. As in previous simulations with the "naked" Dickerson's dodecamer,[18] these systems were then optimized and equilibrated using our standard multistep protocol,[24,25] which lasts for more than 100 ps of restricted and unrestricted MD simulation, plus additional 200 ps of unrestrained MD. The systems were then subject to 10 ns of unrestrained MD simulation in the isothermic–isobaric ensemble (T = 298 K, P = 1 atm). Periodic boundary conditions and the PME method[26] were used to account for long-range interactions. SHAKE[27] was used to maintain all the chemical bonds at their equilibrium distances, which allowed us to use a 2 fs time scale for integration of Newton equations. Global center-of-mass movements were removed every 0.1 ns to avoid artifactual cooling of the system. PARM-98[28,29] and TIP3P (30) forcefields were used to represent molecular interactions. Missing parameters for netropsin, DAPI, and Hoescht 33258 were kindly supplied by S. B. Singh, N. Spackova, and S. Harris and were those used in previous MD simulations of solvated complexes of DNA with these drugs.[31–33]

MD Simulations in the Gas Phase. A crucial decision in these simulations was the assignment of the total charge of the complex and

(19) Drew, H. R.; Wing, R. M.; Takano, T.; Broka, C. Tanaka, S.; Itakura, K.; Dickerson, R. E. *Proc. Natl Acad. Sci. U.S.A.* **1981**, *78*, 2179–2183. PDB Entry 1BNA.
(20) Larsen, R. A.; Goodsell, D. S.; Cascio, D.; Grzeskowiak, K.; Dickerson, R. E. *J. Biomol. Struct. Dyn.* **1989**, *7*, 477–491.
(21) Quintana, J. R.; Lipanov, A. A.; Dickerson, R. *Biochemistry*. **1991**, *30*, 10294–12306.
(22) Sriram, M.; van der Marel, G. A.; Roelen, H. L.; van Boom, J. H.; Wang, A. H. *Biochemistry*. **1992**, *31*, 11823–11834.
(23) Gelpí, J. L.; Kalko, S. G.; Barril, X.; Cirera, J.; de la Cruz, X.; Luque, F. J.; Orozco, M. *Proteins* **2001**, *45*, 428–437.
(24) Shields, G. C.; Laughton, C. A.; Orozco, M. *J. Am. Chem. Soc.* **1997**, *119*, 7563–7469.
(25) (a) Soliva, R.; Laughton, C. A.; Luque, F. J.; Orozco, M. *J. Am. Chem. Soc.* **1998**, *120*, 11226. (b) Shields, G. C.; Laughton, C. A.; Orozco, M. *J. Am. Chem. Soc.* **1998**, *120*, 5895–5904.
(26) Darden, T A.; York, D.; Pedersen, L. *J. Chem. Phys.* **1993**, *98*, 10089–10092.
(27) Ryckaert, J. P.; Ciccotti, G.; Berendsen, H. J. C. *J. Comput. Phys.* **1977**, *23*, 327–341.
(28) Cornell, W. D.; Cieplak, P.; Bayly, C. I.; Gould, I. R.; Merz, K.; Ferguson, D. M.; Spellmeyer, D. C.; Fox, T.; Caldwell, J. W.; Kollman, P. A. *J. Am. Chem. Soc.* **1995**, *117*, 11946–11975.
(29) Cheatham, T. E.; Cieplak, P.; Kollman, P. A. *J. Biomol. Struct. Dyn.* **1999**, *16*, 845–862.
(30) Jorgensen, W. L.; Chandrasekhar, J.; Madura, J. D.; Impey, R. W.; Klein, M. L. *J. Chem. Phys.* **1983**, *79*, 926–935.
(31) Singh, S. B.; Kollman, P. A. *J. Am. Chem. Soc.* **2001**, *123*, 3267–3271.
(32) Spackova, N.; Cheatham, T. E., III; Ryjacek, F.; Lankas, F.; Van Meervelt, L.; Hobza, P.; Sponer, J. *J. Am. Chem. Soc.* **2003**, *125*, 1759–1769.
(33) Harris, S. A.; Gavathiotis, E.; Searle, M. S.; Orozco, M.; Laughton, C. A. *J. Am. Chem. Soc.* **2001**, *123*, 12658–12663.

Table 1. Scheme of the MD Simulations Discussed in This Paper[a]

complex	environment	force field	net charge	temp (K)	neutralization scheme	simulation time (ns)	simulation code
naked[b]	water	P-98	0	298		10	NWL
naked[b]	gas phase	P-98	−6	298		250	NGL
naked[b]	gas phase	P-98	−6	448		100	NGH
DAPI	water	P-98	0	298		10	DW98L
DAPI	gas phase	P-94	−4	298	CD	100	DG94(4)L(CD)
DAPI	gas phase	P-98	−4	298	CD	500	DG98(4)L(CD)
DAPI	gas phase	P-94	−4	448	CD	100	DG94(4)H(CD)
DAPI	gas phase	P-98	−4	448	CD	500	DG98(4)H(CD)
DAPI	gas phase	P-98	−6	298	CD	100	DG98(6)L(CD)
DAPI	gas phase	P-98	−6	298	ND	100	DG98(6)L(ND)
DAPI	gas phase	P-98	−6	448	ND	100	DG98(6)H(ND)
H-33258	water	P-98	0	298		10	HW98L
H-33258	gas phase	P-98	−5	298	CD	500	HG(5)L(CD)
H-33258	gas phase	P-98	−5	448	CD	100	HG(5)H(CD)
H-33258	gas phase	P-98	−6	298	CD	100	HG(6)L(CD)
H-33258	gas phase	P-98	−6	298	ND	100	HG(6)L(ND)
H-33258	gas phase	P-98	−6	448	ND	100	HG(6)H(ND)
netropsin	water	P-98	0	298		10	NW98L
netropsin	gas phase	P-98	−4	298	CD	500	NG(4)L(CD)
netropsin	gas phase	P-98	−4	448	CD	100	NG(4)H(CD)
netropsin	gas phase	P-98	−6	298	CD	100	NG(6)L(CD)
netropsin	gas phase	P-98	−6	298	ND	100	NG(6)L(ND)
netropsin	gas phase	P-98	−6	448	ND	100	NG(6)H(ND)

[a] P-98 and P-94 refer to force field (PARM98 or PARM94) used, and CD and ND, to the neutralization scheme (charged drug or neutral drug). See text for additional details. [b] Trajectories from ref 18.

how the charges are distributed along the molecule. Based on ES experiments of naked and DNA:mG-binder complexes[8−12,14−16] two possibilities can be envisaged: (i) to assign a total charge of −6 for all the complexes or (ii) to assign a charge of −4 for complexes with DAPI and netropsin and −5 for the complex with Hoechst 33258. Our previous study[18] demonstrated that qualitatively similar results are obtained if the charge is distributed uniformly in all the ionizable groups or if it is concentrated in a few ionizable groups selected to minimize the electrostatic repulsion. Accordingly, we decided to use here only the second neutralization procedure, which is closer to chemical intuition. Thus, we simulated using all the possible ways to split a given formal charge into the set of ionizable groups, taking as the real one that showing the best electrostatic interaction energy. Another delicate decision concerned the nature of the ionizable groups. Here two different approaches were adopted: (i) to maintain the charge of the drug (denoted hereafter CD-simulations) in water and neutralize the selected phosphates (by adding a proton, HO1, to the phosphate oxygen O1P) to obtain the desired net charge, and (ii) to neutralize the charge of the drug (ND simulations) by removing the most acidic proton before adjusting the charges of the phosphates. In this latter case RESP/6-31G(d) charges[34] were computed for neutral drugs.

As in our previous work,[18] we decided to carry out simulations at both room (298 K) and high (448 K) temperatures. The first simulations will serve to study ideal vaporization processes, while the second is closer to the real conditions used in ES experiments.[10,11] Finally, following again our previous work,[18] we used the PARM-98 force-field in all cases,[28,29] except for DAPI simulations, where we performed also control simulations with the PARM-94 force-field.[28] Standard charges (without polarity reduction) were used in all cases.[18]

The structures corresponding to the 5 ns point of the MD simulations in water were used as starting conformations for the simulations in vacuo after removing waters and counterions. The structures were modified to fit the conditions of the simulation in the gas phase (see above) and equilibrated at 298 K for 100 ps starting from the velocities of the MD simulation in water. A test calculation was performed (data not shown) dehydrating one of the systems (DAPI) in 6 steps (from bulk to 200 waters, then 100, 50, 25, 10, and vacuum); during each step (0.2 ns long) the temperature was raised 30 K and the charge is reduced. No important differences are found between the normal dehydrated trajectory and that started after the smooth dehydration.

After equilibration of the structures, MD simulations were performed for at least 100 ns at constant temperature (298 K). Three of the simulations (CD simulations with PARM-98 for the three drugs) were extended to 0.5 μs. The structures obtained after 1 ns were then used as starting points for additional MD simulations at 448 K. Heating from 298 to 448 K was performed in 100 ps, and the new MD simulations were run for at least 100 ns. One control simulation (CD simulation using PARM-98 for DAPI) was extended to 0.5 μs. Overall, MD simulations cover more than 3.3 μs of MD simulations of DNA:mG-binders in the gas phase and 30 ns in aqueous solution (see Table 1).

As for the simulations in solution, SHAKE[27] was used to constrain all the bonds, but to avoid instabilities in the trajectories the integration time step was 1 fs. All nonbonded interactions were considered in energy calculations (no cutoff was used). Simulations were performed at constant temperature (T = 298 or 448 K). To guarantee that the thermal energy was not massively used in global movements, we monitored the trajectories and removed the center-of-mass velocity every 1 ns. All simulations were performed using the AMBER 5.1 suite of programs.[35]

Analysis of Trajectories. A large variety of geometrical analyses, including root-mean-square deviations (RMSd), helicity calculations, and energy analysis were performed. Unless otherwise stated, the analysis was performed for 100 structures collected at 9−10 ns of the simulations in water (one structure every 10 ps), and 100 structures collected at 90−100 ns of the simulations in the gas phase (one structure every 100 ps). A local polar coordinate system was defined (see Figure 1) to describe the relative position of the drug with respect to the duplex. Intramolecular contact maps in the DNA were computed as described in our previous work,[18] assuming that a contact between two residues exist when any interatomic distance between them is smaller than 3.5 Å. Drug−DNA contact profiles were computed following the same approach. Solvent accessible surfaces (SASs) were determined using the NACCESS program[36] and considering only DNA atoms or both drug and DNA atoms. To avoid end effects, only the SASs of the central

(34) Bayly, C. E.; Cieplak, P.; Cornell, W. D.; Kollman, P. A. *J. Phys. Chem.* **1993**, *97*, 10269−10280.

(35) Case, D. A. et al. *AMBER 5*; University of California, San Francisco: 1997.

(36) Hubbard, S. J.; J. M. Thornton *NACCESS Computer Program*; Department of Biochemistry and Molecular Biology. University College London: London, U.K., 1993.

10-mer in the dodecamer were computed. Interactions between nucleobases were classified into hydrogen bonding and stacking. Two bases in contact were considered hydrogen-bonded when at least one of these interactions is found (heteroatom−heteroatom distance below 3.5 Å, and deviation of less than 20° from linearity); otherwise the interaction is labeled as "stacking".

Principal component analysis (PCA[37,38]) was used to examine the essential dynamics of DNA (for comparison purposes, covariance matrices were built up excluding the HO1). To avoid end effects, base pairs at 5′ and 3′ were removed from the analysis. In all cases the trajectories were projected along the first modes of motion to discard the existence of Fourier-shaped profiles, which would indicate the existence of massive random movements in the DNA.[39]

The similarity in the dynamical behavior of the duplexes in two trajectories was analyzed by comparing both the flexibility of the molecule along the essential modes and the nature of these essential movements. For this purpose, the force constants associated to the deformation along the softest modes were computed from the eigenvalues obtained by diagonalization of the covariance matrix (see eq 1 and refs 38, 40, 41). We then determined the similarity in the nature of deformation modes by computing the absolute (γ) and relative (κ) similarity indexes[38,40,41] between the first 10 eigenvectors (those which typically describe 80−90% of the positional variance of the trajectories). To make results comparable, indexes γ and κ were computed taking 10 ns (from 0 to 10 ns in water and from 90 to 100 ns in the gas phase) samplings. Note than an index $\kappa = 1.0$ means an identical deformation pattern for two trajectories, while $\kappa = 0.0$ indicates that the movements are orthogonal.

$$K_i^{\mathrm{A}} = k_{\mathrm{B}}T/\lambda_i \tag{1}$$

where K_i^{A} is the force constant associated to the deformation mode i in trajectory A, k_{B} is Boltzman's constant, T is the absolute temperature, and λ_i is one eigenvalue (in Å^2) obtained by diagonalization of the Cartesian covariance matrix (let us note that force constants should in principle be independent of the simulation if the molecule moves in the harmonic regime at different T).

$$\gamma_{AB} = \frac{1}{n}\sum_{j=1}^{n}\sum_{i=1}^{n}(\nu_i^A \cdot \nu_j^B)^2 \tag{2}$$

$$\kappa_{AB} = 2\frac{\gamma_{AB}}{(\gamma_{AA}^T + \gamma_{BB}^T)} \tag{3}$$

where ν are principal component ($3 \times N$ dimensional, with $N =$ number of atoms) vectors, A and B stand for two different trajectories of equal length, and the self-similarity indexes γ_{AA}^T and γ_{BB}^T are obtained by using eq 3 for the same trajectories using two nonoverlapping portions of equal time length.

Manipulation of the force constants associated with the eigenvectors allowed us[42] to determine a qualitative measure of the accessible conformational volume for a molecule in the harmonic approach (see eq 4). Larger conformational spaces will be associated with more flexible structures. However, a more complete picture of the different flexibility of structures can be obtained by intramolecular entropy calculations performed following Schlitter's or Andricioaei and Karplus methods,[43,44] which were computed for both gas phase and solution simulations using 10 ns samplings (0 to 10 ns in water and 90−100 ns in gas phase) and later extrapolated to infinite simulation time using Harris's et al. procedure.[33]

$$V = \prod_{i=1}^{m}(1 + \lambda_i)^{1/2} \tag{4}$$

where m stands for the total number of eigenvectors (i.e., the dimension of the covariance matrix).

MD simulations were evaluated to predict the cross sections expected for the different complexes. The cross section is a low resolution structural parameter that can be experimentally derived and provides a low resolution picture of the general structure shape of the molecule.[17,45−49] Calculations were performed using the SIGMA program developed by Bower's group and provided by Dr. Wyttenbach[45−47] using a Lennard−Jones collision model. We averaged the values for 100 snapshots collected during the 9−10 ns period of aqueous simulations, and 90−100 ns period of the gas phase ones. The Monte Carlo procedure used to compute the cross sections[17,45−47] was performed until a convergence better than 1% was achieved. Selected conformations were also studied using the much more CPU-demanding methodology developed by Jarrold and co-workers,[48,49] as implemented in the MOBCAL/PA approach (available at the web site http://nano.chem.indiana.edu/software.html). In general, good qualitative agreement was found between the results obtained from the two approaches.

Results and Discussion

MD Simulations in Water. Simulations provide stable trajectories for all the drug−DNA complexes at room temperature, with small deviations from either the experimental structure (RMSd varying from 1.6 to 1.8 Å; see Table 2) or the MD-averaged conformation determined for each simulation (RMSD ranging from 1.2 to 1.8 Å; see Table 2 and Table S1 in the Supporting Information). In fact, the small RMSDs from the MD-averaged conformation indicate that a narrow region of the conformational space is sampled in the simulations. Interestingly, the binding of the drugs does not introduce major distortions in the geometry of the duplex, as noted in the small RMSD values determined between the structures of the drug−DNA complex collected during the trajectories and the MD-averaged conformation of the naked DNA in aqueous solution (RMSD ranging from 2.7 to 3.0 Å; see Table 2).

Helical analysis (data not displayed), DNA−DNA contact maps (see Figure 2 and Supporting Information, Figure S1), the SAS of DNA determined in the absence of drug (SAS ranging from 3591 to 3635 Å^2; see Table 3 and Table S2 in the Supporting Information), and theoretical collision cross sections (values between 912 and 925 Å^2; see Table 3) show that there are no major alterations in the structure of the duplex upon binding to mG-binders and that all structures sample the B-region of the conformational space, with all the sugars in the *South* and *South-East* puckerings.

As found in previous aqueous MD simulations of related systems,[31−33] the drugs do not experience substantial fluctuations

(37) Sherer, E.; Harris, S. A.; Soliva, R.; Orozco, M.; Laughton, C. A. *J. Am. Chem. Soc.* **1999**, *121*, 5981−5991.
(38) Orozco, M.; Perez; Noy, A.; Luque, F. J. *Chem. Soc. Rev.* **2003**, *32*, 350−364.
(39) Hess, B. *Phys. Rev. E.* **2000**, *62*, 8438−8448.
(40) Noy, A.; Pérez, A.; Lankas; F.; Luque, F. J.; Orozco. M. *J. Mol. Biol.* **2004**, *343*, 627−638.
(41) Pérez, A.; Noy, A.; Lankas, F.; Luque, F. J.; Orozco, M. *Nucleic Acids Res.* **2004**, *32*, 6144−6151.
(42) Blas, J. R.; Pérez, A.; Rueda, M.; Luque, F. J.; Orozco, M. *J. Chem. Theory Comput.*, submitted.
(43) Schlitter, J. *Chem. Phys. Lett.* **1993**, *215*, 617−621.
(44) Andricioaei, I.; Karplus, M. *J. Chem. Phys.* **2001**, *115*, 6289−6292.
(45) Von Helden, G.; Hsu, M.; Gotts, N.; Bowers, M. T. *J. Phys. Chem.* **1993**, *97*, 8182−8192.
(46) Wyttenbach, T.; von Helden, G.; Batka, J. J.; Carlat, D.; Bowers, M. T. *J. Am. Soc. Mass Spectrom.* **1997**, *8*, 275−282.
(47) Wyttenbach, T.; Witt, M.; Bowers, M. T. J. *Am. Chem. Soc.* **2000**, *122*, 3458−3464.
(48) Shvartsburg, A. A.; Jarrold, F. *Chem. Phys. Lett.* **1996**, *261*, 86−91.
(49) Mesleh, M. F.; Hunter, J. M.; Shvartsburg, A. A.; Schwartz, G. C.; Jarrold, M. F. *J. Phys. Chem.* **1996**, *100*, 16082−16086.

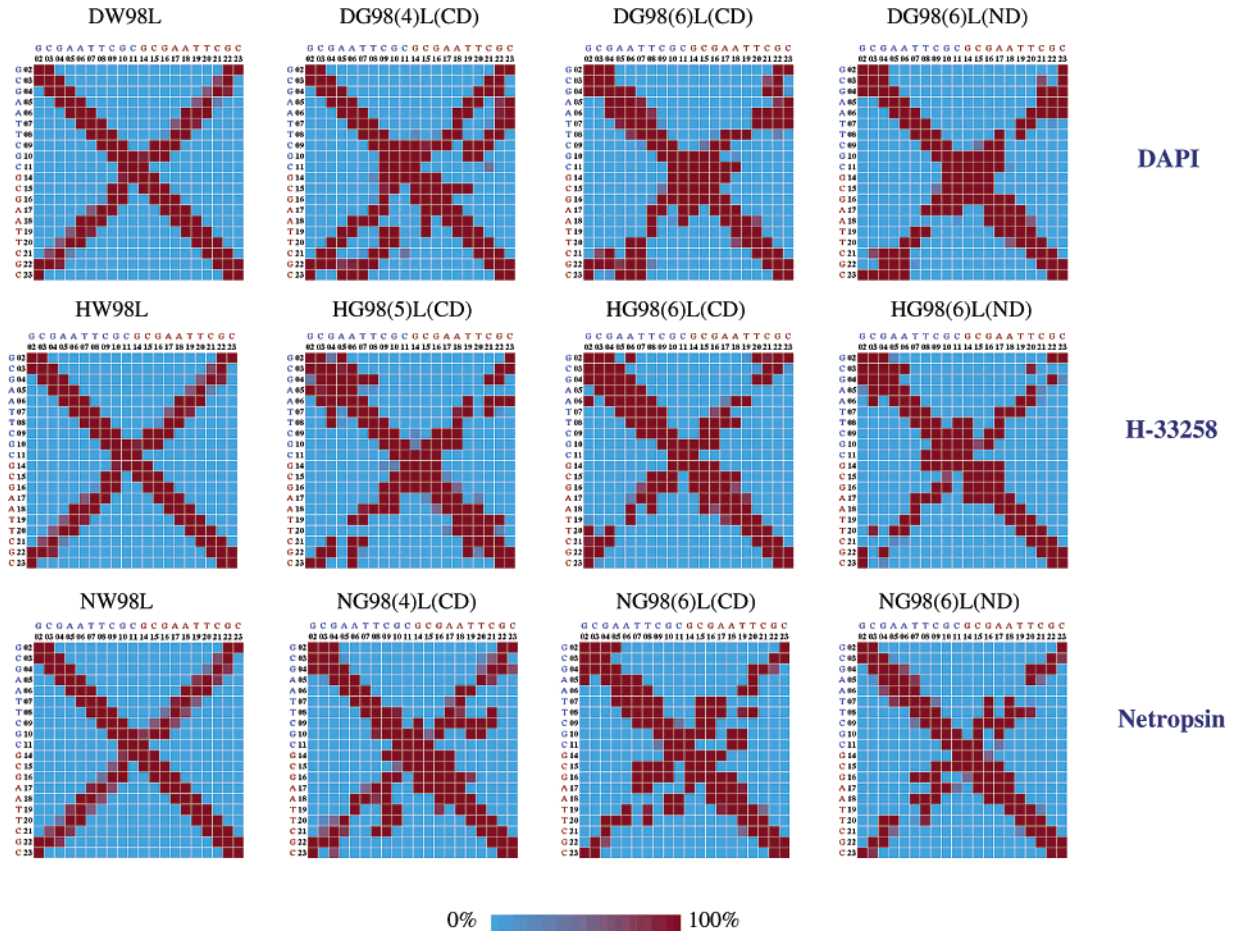

Figure 2. DNA−DNA contact maps (see Methods) for DNA in different simulations.

Table 2. Mass-Weighted All-Atom Root Mean Square Deviations (RMSD; in Å) for the MD Trajectories Determined with Respect to Several Reference Conformations[a]

complex	code	RMSD(cryst)	RMSD(avg)	RMSD(MD_{aq})
naked	**NWL**	**1.8 (0.4)**	**1.3 (0.3)**	**1.3 (0.3)**
naked	NGLg	8.2 (0.4)	2.4 (0.8)	9.1 (0.4)
naked	NGHg	7.2 (0.4)	1.7 (0.7)	7.6 (0.3)
DAPI	**DW98L**	**1.6 (0.3)**	**1.2 (0.2)**	**2.7 (0.2)**
DAPI	DGLg	7.5−8.1 (0.2−0.8)	1.6−2.4 (0.8−1.4)	8.1−9.0 (0.2−0.7)
DAPI	DGHg	6.8−9.8 (0.2−0.5)	1.5−2.8 (0.8−1.3)	6.6−9.7 (0.2−0.5)
H-33258	**HW98L**	**1.8 (0.3)**	**1.3 (0.3)**	**2.8 (0.2)**
H-33258	HGLg	6.1−7.7 (0.3−1.7)	0.9−4.5 (0.6−3.0)	6.4−8.0 (0.2−1.4)
H-33258	HGHg	8.2−10.0 (0.4−0.8)	2.3−3.1 (1.0−1.7)	8.0−9.5 (0.3−0.6)
netropsin	**NW98L**	**1.7 (0.3)**	**1.8 (0.4)**	**3.0 (0.2)**
netropsin	NGLg	5.6−7.5 (0.3−0.7)	0.7−2.5 (0.5−1.1)	6.1−7.5 (0.2−0.7)
netropsin	NGHg	7.3−8.0 (0.4−0.6)	2.7−2.9 (1.2−1.5)	6.9−7.8 (0.3−0.4)

[a] The corresponding crystal structure (cryst; PDB codes 355D (naked), 1d30 (DAPI), 1d43 (Hoechst 33258), and 1d86 (Netropsin)). The MD averaged conformation obtained for each MD simulation (avg). The MD-averaged conformation obtained from the simulation of the naked DNA in solution (MD_{aq}). Standard deviations (in Å) are shown in parentheses. Control simulations in water are displayed in bold. For gas phase simulations only ranges are shown for high and low temperature runs. The individual values are available in Table S1 of the Supporting Information.

with respect to their initial placements in the minor groove. This is noted in the relative position and orientation of the drug with respect to the DNA (average drug−DNA distance ranging from 5.9 to 6.9 Å and angle varying from 36.8° to 39.3°; see Figure 1 and Table 4) and in the drug−DNA contact profiles, which are very similar irrespective of whether they are averaged from the snapshots collected along the trajectories or computed for the corresponding crystal structures (see Supporting Information, Figure S-6). Binding of the drug slightly reduces the flexibility of the duplex,[33] as noted in the decrease of both the generalized configurational volumes (see Figure 3 and eq 4) and the duplex entropy (by 0.1−0.2 kcal/mol K; see Table 5). In agreement with such a reduction in the flexibility of the duplex, the force constants associated with the first deformation modes tend to increase upon drug binding relative to the naked DNA (see Supporting Information Table S3). However, the nature of such deformations in naked and drug-bound DNAs is very similar, as noted in similarity indexes κ (see eq 3) around 0.9 between bound and unbound duplexes (see Table 6).

In summary, current "state-of-the-art" MD simulations are able to reproduce accurately the key characteristics of the three DNA-drug complexes in aqueous solution at room temperature.

Table 3. DNA-Solvent Accessible Surfaces (SAS for Central 10 mer) and Collision Cross Sections (both in Å^2) for Different Simulations (and Corresponding Standard Deviations) and Reference Fiber Helices[a]

complex	code	SAS no drug	SAS with drug	ΔSAS	cross section
B-DNA	*B-DNA*	*3268*			*907 (18)*
A-DNA	*A-DNA*	*3491*			*823 (19)*
naked	**NWL**	**3593 (22)**			**912 (19)**
naked	NGL	3359 (29)			899 (27)
naked	NGH	2899 (61)			775 (21)
DAPI	**DW98L**	**3608 (24)**	**3355 (22)**	**253**	**912 (19)**
DAPI	DGLg	3025−3216 (22−44)	2856−2991 (23−41)	168−225	773−866 (20−23)
DAPI	DGHg	2738−3127 (31−44)	2566−2946 (30−41)	171−192	725−824 (15−21)
H-33258	**HW98L**	**3591 (17)**	**3256 (24)**	**335**	**916 (17)**
H-33258	HGLg	3127−3307 (24−41)	2858−2973 (28−77)	253−333	829−872 (17−31)
H-33258	HGHg	2906−2985 (44−67)	2607−2713 (41−52)	271−299	754−758 (16−17)
netropsin	**NW98L**	**3635 (28)**	**3316 (32)**	**318**	**925 (27)**
netropsin	NGLg	2838−3388 (35−45)	2554−3091 (33−46)	284−296	755−861 (17−25)
netropsin	NGHg	2622−3288 (51−59)	2399−2972 (49−63)	223−315	705−844 (11−29)

[a] SAS calculations were performed considering only the DNA (no-drug values) as well as including the drug. Calculations were performed using 100 snapshots collected along 9−10 ns (water) or 90−100 ns (vacuum) of the trajectories or from 100 replicas of reference fiber structures. For gas phase simulations only ranges are shown for high and low temperature runs. The individual values are available in Table S2 of the Supporting Information.

Table 4. Geometrical Parameters (and Associated Standard Deviations) Related to the Position of the Drug with Respect to DNA[a]

complex	simulation	distance COM to DNA *z*-axis	DNA–drug *Z*-axis angle
DAPI	**DW98L/*crystal***	**6.3 (0.2)/*5.5***	**39.3 (2.2)/*38.4***
DAPI	DG94(4)L(CD)	1.8 (0.2)	33.3 (1.6)
DAPI	DG98(4)L(CD)	0.6 (0.2)	10.3 (1.3)
DAPI	DG94(4)H(CD)	1.6 (0.2)	33.4 (1.5)
DAPI	DG98(4)H(CD)	1.3 (0.1)	24.3 (2.2)
DAPI	DG98(6)L(CD)	4.0 (0.3)	12.7 (1.4)
DAPI	DG98(6)L(ND)	2.6 (0.3)	47.1 (1.6)
DAPI	DG98(6)H(ND)	5.6 (0.6)	41.4 (20.3)
H-33258	**HW98L/*crystal***	**5.9 (0.4)/*4.8***	**39.0 (2.6)/*39.1***
H-33258	HG(5)L(CD)	3.8 (0.4)	29.6 (2.6)
H-33258	HG(5)H(CD)	3.9 (0.2)	23.2 (3.1)
H-33258	HG(6)L(CD)	5.2 (0.3)	46.2 (3.0)
H-33258	HG(6)L(ND)	2.4 (0.4)	46.8 (1.6)
H-33258	HG(6)H(ND)	5.3 (0.2)	27.1 (3.2)
netropsin	**NW98L/*crystal***	**6.9 (0.4)/*5.3***	**36.8 (4.6)/*36.1***
netropsin	NG(4)L(CD)	2.7 (0.1)	25.5 (1.6)
netropsin	NG(4)H(CD)	7.7 (0.5)	35.5 (6.1)
netropsin	NG(6)L(CD)	4.1 (0.4)	22.2 (1.5)
netropsin	NG(6)L(ND)	0.6 (0.4)	98.6 (8.2)
netropsin	NG(6)H(ND)	7.6 (0.6)	78.6 (9.5)

[a] For description of the different parameters see Methods and Figure 1. Distances are in Å, and angles, in degree. COM stands for center of mass of the drug. Values obtained for the crystal are displayed in italics.

Moreover, as suggested by previous authors,[31−33] the interaction of mG-binders with DNA produces only subtle distortions in the structure and dynamics of the duplex, at least for Dickerson's dodecamer.

MD Simulations in the Gas Phase. Upon partial charge neutralization and vaporization the drug−DNA complexes show a large conformational transition, as noted in very large RMSDs with respect to the solvated structures (RMSDs ≥ 6.1 Å; see Table 2 and also Supporting Information Table S1) and to the crystal structures (RMSDs ≥ 5.6 Å; see Table 2 and also Supporting Information Table S1). Such a transition occurs in the very first nanosecond of the trajectory (see Figure 4). For some complexes small transitions are detected during the first 50 ns, but after that period the structures remain quite stable. In fact, the analysis of 0.5 μs and 0.1 μs MD simulations show RMSDs with respect to the respective MD-average conformations which are similar or even smaller than those obtained for the corresponding simulations in water (see Table 2).

Though vaporization promotes a large conformational change in the helix, it does not lead to an unfolding transition to a random coil structure, as noted in the structures shown in Figure 5 (see also Supporting Information Figure S2). Different trajectories lead to a variety of average structures even for the same drug, suggesting that the complex can be trapped in different conformations depending on experimental conditions (see Figure 5). However, some common trends can be identified. First, as those found in previous studies of naked DNAs,[17,18] no strand dissociation events are detected even for the 0.5 μs MD trajectories at 448 K. Second, despite the structural distortions, the duplexes maintain a certain degree of helicity, especially those bearing the smallest formal charge, as noted in the DNA−DNA contact maps (see Figure 2 and also Supporting Information S1) and in the MD-averaged conformations obtained in the last 10 ns of each gas phase trajectory (see Figure 5 and also Supporting Information Figure S2).

DNA−DNA contact maps (see Figure 2) show the existence of many residue−residue contacts in the gas phase. In fact, upon transfer to the gas phase there is a notable compression of the duplex, which decreases the SAS (determined in the absence of the drug) by 10−30% relative to the values found in solution (see Table 3). As a result of the tight packing of DNA, there is a large amount of hydrogen-bonded and stacking interactions between nucleobases. Thus, at room temperature the gas phase duplexes contain 40−50% of the nucleobase−nucleobase hydrogen bonding found in aqueous solution (20−30% at 448 K). These percentages, however, are systematically smaller than those found in naked DNA, thus suggesting that the drug disturbs hydrogen bonding between nucleobases in the gas phase. As found in previous simulations of naked DNA,[18] hydrogen bonds in A−T steps are generally more labile than those in G−C ones, which are quite well preserved in the gas phase. Furthermore, a large number of noncanonical hydrogen bonds are formed, not only between complementary pairs, but also with other nucleobases. There are many stacking interactions between nucleotides, including noncanonical T-shape contacts and clusterings involving three nucleobases. In fact, the stacking energy in the gas phase at 298 K is around 70% of that found in aqueous solution, confirming[18] that transfer to the gas phase does not dramatically decrease the magnitude of nucleobase−nucleobase stacking.

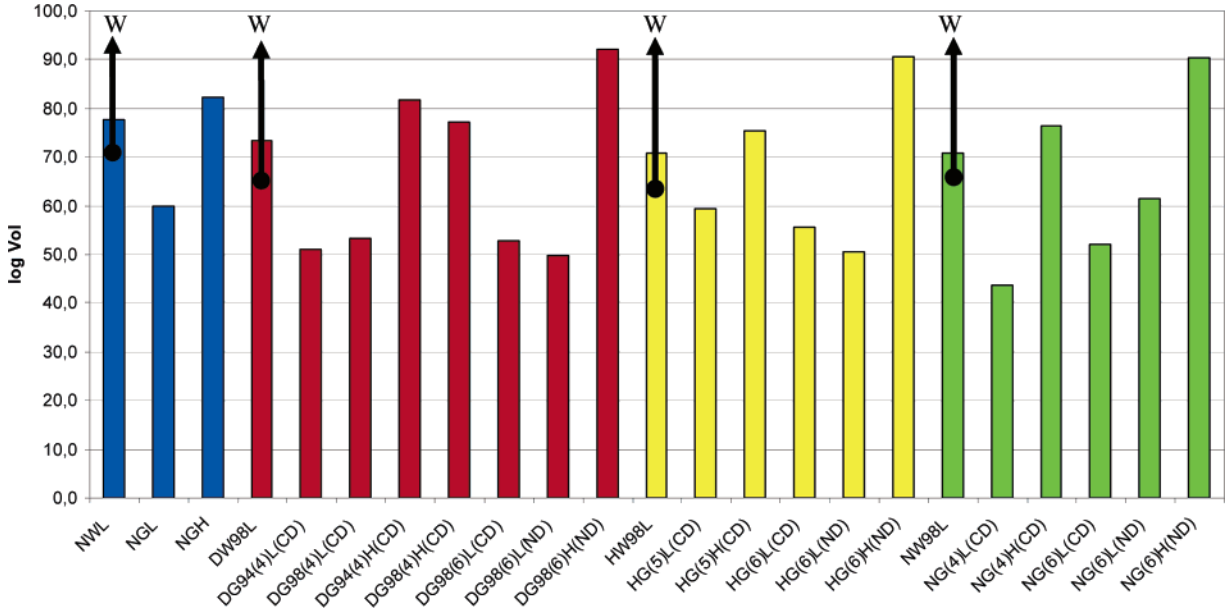

Figure 3. Logarithm of the generalized configurational volume (see eq 4) for the DNA in the different simulations. For discussion purposes, aqueous simulations are marked with an arrow.

Table 5. DNA Intramolecular Entropy (in kcal/mol K) Computed from Schlitter and Andricioaei−Karplus for the Different Simulations[a]

		Schlitter		Andricioaei–Karplus	
complex	simulation	$S(t = 10$ ns)	$S(t = \infty)$	$S(t = 10$ ns)	$S(t = \infty)$
naked	**NWL**	**2.0**	**2.4 (0.0)**	**1.9**	**2.0 (0.0)**
naked	NGL	1.7	2.0 (0.0)	1.6	1.7 (0.0)
naked	NGH	2.4	3.2 (0.1)	2.3	2.7 (0.1)
DAPI	**DW98L**	**1.9**	**2.3 (0.0)**	**1.8**	**1.9 (0.0)**
DAPI	DG94(4)L(CD)	1.7	1.9 (0.0)	1.5	1.6 (0.0)
DAPI	DG98(4)L(CD)	1.7	2.1 (0.1)	1.6	1.7 (0.1)
DAPI	DG94(4)H(CD)	2.4	3.3 (0.1)	2.3	2.7 (0.0)
DAPI	DG98(4)H(CD)	2.4	3.4 (0.3)	2.3	2.7 (0.1)
DAPI	DG98(6)L(CD)	1.7	1.9 (0.0)	1.5	1.6 (0.0)
DAPI	DG98(6)L(ND)	1.6	1.9 (0.0)	1.5	1.6 (0.0)
DAPI	DG98(6)H(ND)	2.6	3.4 (0.1)	2.4	2.8 (0.1)
H-33258	**HW98L**	**1.9**	**2.2 (0.0)**	**1.8**	**1.9 (0.0)**
H-33258	HG(5)L(CD)	1.7	2.1 (0.0)	1.6	1.7 (0.0)
H-33258	HG(5)H(CD)	2.4	3.2 (0.2)	2.2	2.6 (0.1)
H-33258	HG(6)L(CD)	1.7	2.1 (0.2)	1.6	1.7 (0.1)
H-33258	HG(6)L(ND)	1.6	1.9 (0.0)	1.5	1.6 (0.0)
H-33258	HG(6)H(ND)	2.6	3.5 (0.2)	2.4	2.9 (0.1)
netropsin	**NW98L**	**1.9**	**2.3 (0.1)**	**1.8**	**1.9 (0.0)**
netropsin	NG(4)L(CD)	1.6	1.8 (0.0)	1.4	1.5 (0.0)
netropsin	NG(4)H(CD)	2.4	3.1 (0.1)	2.2	2.6 (0.1)
netropsin	NG(6)L(CD)	1.7	2.0 (0.0)	1.5	1.6 (0.0)
netropsin	NG(6)L(ND)	1.7	2.1 (0.0)	1.6	1.7 (0.0)
netropsin	NG(6)H(ND)	2.5	3.5 (0.2)	2.4	2.8 (0.1)

[a] Values obtained for 10 ns and extrapolated to infinite simulation time (with associated standard errors) are displayed.

Collision cross sections of naked DNA at room temperature are slightly lower than those found in aqueous solution, taking values typical of a B-like helix (see Table 3), while raising the temperature displaces the cross section to values closer to those of an A-like helix (see Table 3 and also Supporting Information Table S2). Similar cross sections are found in drug−DNA simulations in the gas phase irrespective of the nature of the drug, temperature, force-field, total charge, and neutralization scheme (see Table 3). At least for the 12-mer duplex studied here, the values are generally close to those expected for an A-type helix, a finding that might be attributed to the slight compression of the DNA upon transfer to the gas phase (see above).

Both the estimated entropies and the generalized configurational volumes (see Table 5 and Figure 3) confirm that vaporization does not lead to a transition from structured to random coil conformations. In fact, at a given temperature there is a reduction in the flexibility of the duplex upon vaporization, as noted in the decrease in the entropy and the generalized configurational space irrespective of the force field, nature of the drug, global charge, and neutralization protocol (see Table 5 and Figure 3). The decrease in flexibility upon vaporization is also reflected in a general (temperature independent) increase in the force constants associated to harmonic deformations along essential movements (see Supporting Information Table S3).

The type of essential movements of the DNA strands in DNA−drug complexes in the gas phase and in solution is quite different (see κ indexes in Table 6). Furthermore, the nature of such movements is different for each drug−DNA complex and for each simulation condition and also changes with respect to those happening in naked DNA. However, let us stress that similarity indexes (κ) in the range 0.2−0.4 are impossible to be obtained randomly when only 10 eigenvectors are considered in the calculation (see Discussion in ref 18). This indicates that the DNA strands in the drug−DNA complexes in vacuo maintain some memory of their natural movements in aqueous solution, in agreement with previous findings for simulations of naked DNA in the gas phase.[18]

Irrespective of the simulation conditions, all the drugs appear to be firmly bound to the duplex after 0.1 or 0.5 μs of MD simulations. In other words, 17 independent MD trajectories covering more than 3 μs of unrestrained MD simulations strongly suggest that the drug−DNA complex is stable in the gas phase, at least in the microsecond time scale. This finding, which seems to be against chemical intuition, agrees perfectly with ES experiments (see Introduction) and suggests that the drug−DNA complex is trapped in a conformation which avoids the dissociation of drug and DNA strands.

The SAS occluded by the drug in the gas phase simulations is generally smaller than the occlusion found in water (see Table 3), suggesting that the drug becomes closer to the DNA structure

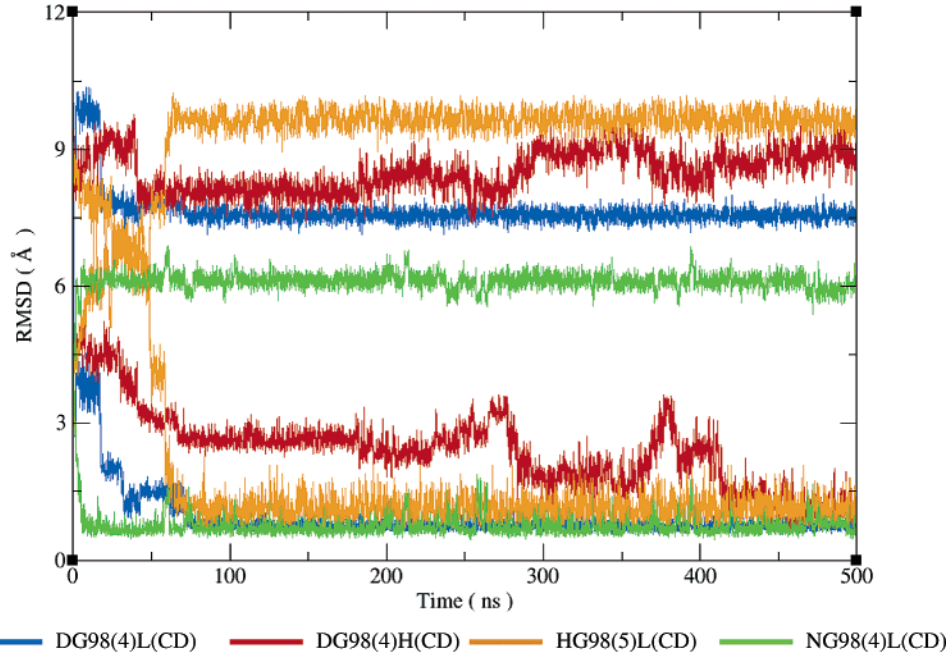

Figure 4. RMS deviations (in Å) from the crystal structure (values in the top of the plot) and the MD-averaged structures (values in the bottom of the plot) for the 0.5 ms trajectories. For clarity, in this case average structures were computed from the 450−500 ns trajectories.

Table 6. Relative Similarity Indexes (κ; See Eq 3) between the DNA Strands in the Different MD Trajectories

NWL	NGL	NGH	DW98L	DG94(4)L(CD)	DG98(4)L(CD)	DG94(4)H(CD)	DG98(4)H(CD)	DG98(6)L(CD)	DG98(6)L(ND)	DG98(6)H(ND)	HW98L	HG(5)L(CD)	HG(5)H(CD)	HG(6)L(CD)	HG(6)L(ND)	HG(6)H(ND)	NW98L	NG(4)L(CD)	NG(4)H(CD)	NG(6)L(CD)	NG(6)L(ND)	NG(6)H(ND)	
1.0	0.4	0.3	1.0	0.2	0.1	0.2	0.2	0.3	0.4	0.3	1.0	0.2	0.2	0.3	0.4	0.2	1.0	0.2	0.1	0.2	0.4	0.2	**NWL**
	1.0	0.3	0.4	0.3	0.2	0.3	0.2	0.4	0.4	0.3	0.4	0.2	0.2	0.1	0.3	0.2	0.4	0.4	0.2	0.2	0.3	0.1	NGL
		1.0	0.3	0.3	0.2	0.3	0.3	0.3	0.3	0.2	0.3	0.2	0.1	0.2	0.2	0.2	0.3	0.2	0.1	0.2	0.2	0.1	NGH
			1.0	0.2	0.1	0.2	0.2	0.3	0.4	0.3	1.0	0.2	0.2	0.3	0.3	0.2	0.9	0.2	0.1	0.2	0.4	0.2	**DW98L**
				1.0	0.3	0.4	0.4	0.3	0.4	0.2	0.2	0.2	0.2	0.1	0.2	0.1	0.3	0.3	0.1	0.2	0.2	0.1	DG94(4)L(CD)
					1.0	0.2	0.3	0.2	0.2	0.2	0.1	0.1	0.1	0.1	0.1	0.1	0.2	0.2	0.1	0.1	0.1	0.1	DG98(4)L(CD)
						1.0	0.3	0.3	0.3	0.3	0.3	0.1	0.2	0.2	0.2	0.2	0.2	0.2	0.1	0.1	0.2	0.1	DG94(4)H(CD)
							1.0	0.2	0.2	0.3	0.2	0.1	0.2	0.2	0.1	0.1	0.2	0.2	0.2	0.2	0.2	0.1	DG98(4)H(CD)
								1.0	0.5	0.3	0.3	0.2	0.2	0.1	0.3	0.1	0.3	0.3	0.1	0.3	0.2	0.1	DG98(6)L(CD)
									1.0	0.4	0.4	0.3	0.2	0.2	0.4	0.2	0.4	0.4	0.1	0.3	0.3	0.2	DG98(6)L(ND)
										1.0	0.3	0.2	0.2	0.2	0.2	0.2	0.3	0.2	0.2	0.2	0.2	0.2	DG98(6)H(ND)
											1.0	0.2	0.2	0.3	0.3	0.2	0.9	0.2	0.1	0.2	0.4	0.2	**HW98L**
												1.0	0.5	0.2	0.2	0.2	0.1	0.1	0.2	0.2	0.2	0.2	HG(5)L(CD)
													1.0	0.2	0.2	0.1	0.2	0.1	0.2	0.1	0.1	0.2	HG(5)H(CD)
														1.0	0.3	0.2	0.3	0.2	0.1	0.2	0.4	0.3	HG(6)L(CD)
															1.0	0.3	0.4	0.3	0.1	0.3	0.3	0.3	HG(6)L(ND)
																1.0	0.2	0.1	0.1	0.2	0.2	0.2	HG(6)H(ND)
																	1.0	0.2	0.2	0.2	0.4	0.2	**NW98L**
																		1.0	0.1	0.2	0.2	0.1	NG(4)L(CD)
																			1.0	0.1	0.1	0.1	NG(4)H(CD)
																				1.0	0.2	0.2	NG(6)L(CD)
																					1.0	0.4	NG(6)L(ND)
																						1.0	NG(6)H(ND)

upon vaporization. Thus, the distance between the center-of-mass of the drug and the *z*-axis of the DNA is drastically reduced in all the gas phase simulations at room temperature (see Table 4) and only increases very slightly in two simulations for netropsin at high temperature. The angle between the DNA and the drug is in most cases similar for the complexes in the gas phase and in aqueous solution. The relative positioning of the drug in the duplex changes upon transfer to the gas phase, but not dramatically. Thus, drug−DNA contact maps (see Supporting Information Figure S3) demonstrate that the drug interacts with a larger number of residues, though there is still a clear preference to interact with the target residues in aqueous simulations. The interaction pattern between the drug and DNA in the gas phase is very complex and obviously depends on the charged state of the DNA and drugs, as well as on the temperature. Nevertheless, when results from the different simulations are analyzed a percentage of drug−DNA hydrogen bonding ranging from 80% (netropsin) to 120% (DAPI) of those found in the aqueous simulations are found for the same complex in the gas phase. Overall, these findings point out the existence of a surprising structural memory in the drug−DNA complex upon transfer from water to the gas phase.

Conclusions

We present here the first systematic analysis of the structure, energetics, and dynamics of noncovalent complexes of DNA

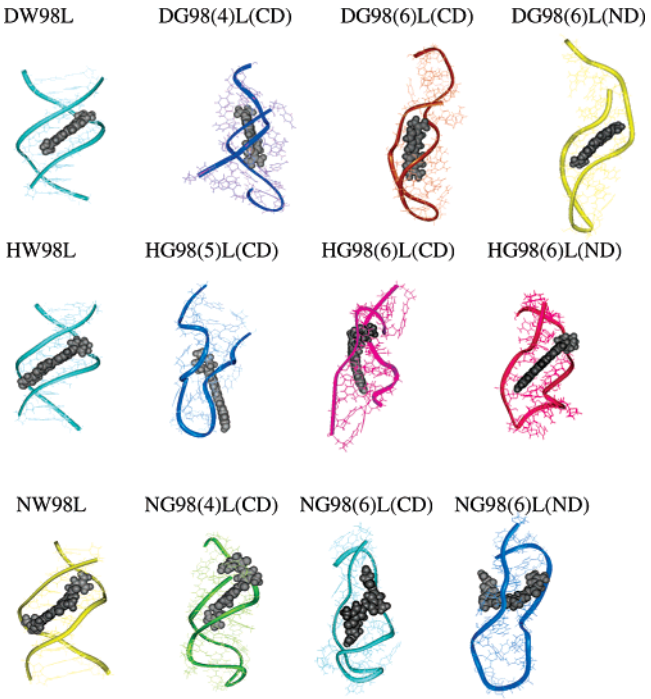

Figure 5. MD-averaged structures representative of the different trajectories studied here. The drug is represented in all the cases using a CPK model.

with mG-binders in the gas phase under conditions similar to those used in ES experiments. As found in shorter simulations of naked DNA, vaporization does not lead to separation of the two DNA strands, though there is a dramatic distortion in the structure of the duplex. Despite such structural distortion, many nucleobase−nucleobase interactions persist, including a non-negligible amount of hydrogen bonding. In general, the DNA strand maintains a pseudo-helical structure, whose structural and dynamical properties have some resemblance with those found in the duplex in aqueous solution. Vaporization does not produce the dissociation of the drug from the DNA, at least in the microsecond time scale. The relative arrangement of the drug with respect to the DNA changes, but there is a clear memory of the original placement of the drug in solvated environments. Despite the logical uncertainties related to the shortcoming of current classical MD simulations, and those arising from the difficulties in reproducing the real experimental conditions inside the spectrometer, present microsecond-time-scale simulations provide valuable information of which can be the nature of dehydrated macromolecules in electrospray experiments.

Acknowledgment. We are indebted to Prof. E. Giralt for many helpful discussions, Dr. Wyttenbach for a copy of SIGMA, and Jarrold's group for a copy of MOBCAL. We thank Drs. S. B. Singh, N. Spackova, and S. Harris for force-field parameters for the drugs. We also thank the computational support of the Centre de Supercomputació de Catalunya (CESCA) and the Centre de Paralelisme de Barcelona (CIRI-CEPBA). This work has been supported by the Spanish DGCYT (BIO2003-06848 and SAF2002-04282), the Fundación BBVA, and the Fundació La Caixa. M.R. is a predoctoral fellowship of the Spanish Ministry of Education and Science.

Supporting Information Available: Supporting Information available: Complete versions of Tables 2 and 3 (Tables S1 and S2). Complete Figures 2 and 5 (Figures S1 and S2). Table S3 and Figure S3. Complete ref 35. This material is available free of charge via the Internet at http://pubs.acs.org.

JA0422110